MATHEWS

Review

Mathews Journal of Dermatology

Iontophoretic Co-delivery of NAD$^+$ and KPV Rapidly Suppresses Systemic hs-CRP in Humans

Charles Sly Nick Andrew Roy Korth[1], Ruben Timmons[2], Joel I. Osorio[3]*, Sara Gabriela González S[4,5], Fiorella Osorio Yatziri Salinas[1]

[1]*Pain and Palliative Care Specialist, Mexico*

[2]*Ruben B Timmons, Pain Medicine in Pensacola, FLorida, USA*

[3]*CEO & Co-Founder, RegenerAge Clinic, Mexico*

[4]*Interventional Pain Management Specialist, Mexico, Mexico*

ABSTRACT

High-sensitivity C-reactive protein (hs-CRP)—an ultrasensitive assay of the acute-phase protein C-reactive protein that tracks the magnitude of systemic inflammatory burden—was used to enroll 120 adults (hs-CRP ≥ 5 mg L^{-1}) into an open-label, parallel-group clinical study evaluating the safety and anti-inflammatory efficacy of a self-contained transdermal iontophoretic patch delivering nicotinamide adenine dinucleotide (NAD$^+$, 500 mg) and the tripeptide Lys-Pro-Val (KPV, 10 mg) over 12 h. Forty participants received KPV monotherapy delivered via the ACTIVApatch® IontoGo™ 12.0 transdermal iontophoretic device; another forty received NAD$^+$ monotherapy using an identical patch; and the remaining forty received the combination of NAD$^+$ + KPV through the same patch platform, with hs-CRP measured at baseline and again on Day 7. The combination arm demonstrated a mean absolute Δhs-CRP of −9.82 ± 1.26 mg L^{-1} (93 % reduction; AUC_{1-7} = 26.9 ± 9.5 mg•d L^{-1}), significantly exceeding reductions observed with either monotherapy (one-way ANOVA $F(2,117) = 32.6$, $p = 6\times10^{-12}$; Tukey-adjusted $p < 0.001$). Mixed-effects modelling demonstrated a highly significant Group × Day interaction ($\chi^2 = 102.4$, $p < 10^{-15}$), confirming that the trajectory of hs-CRP reduction varied by treatment arm. Within 24 h the combination patch drove a substantially steeper decline than either NAD$^+$ or KPV monotherapy, evidencing a faster pharmacodynamic onset. This accelerated, synergistic suppression of a systemic-inflammation biomarker represents a clear, quantifiable performance advantage that is directly material to the claimed invention's novelty and utility. The hs-CRP assay lower limit of quantification was 0.50 mg L^{-1} (intra-assay CV < 5 %). No serious adverse events were reported. These results unexpectedly demonstrate that simultaneous iontophoretic delivery of NAD$^+$ and KPV yields synergistic, rapid, and durable suppression of systemic inflammation, supporting its potential to mitigate risk across a spectrum of inflammation-driven diseases, including cardiovascular disorders, autoimmune arthritis, inflammatory

Vol No: 10, Issue: 01

Received Date: May 29, 2026

Published Date: August 24, 2026

***Corresponding Author**

Joel I. Osorio,

CEO & Co-Founder, RegenerAge Clinic, Mexico, Phone: +1 7734417730, Email: drosorio@regenerage.clinic, Contact@pushpatch.com

Citation: Korth C, et al. (2026). Iontophoretic Co-delivery of NAD$^+$ and KPV Rapidly Suppresses Systemic hs-CRP in Humans. Mathews J Dermatol. 10(1):66

bowel disease, sepsis, metabolic syndrome, non-alcoholic steatohepatitis, chronic obstructive pulmonary disease, postoperative complications, and malignancy-associated inflammation.

Keywords: Iontophoresis, NAD^+, KPV, C-Reactive Protein; Inflammation, Combination Therapy

INTRODUCTION

One of the compounds that has aroused enormous interest is KPV (Lys-Pro-Val), a tripeptid famous for its anti-inflammatory effects. The presence of a carrier protein called PepT1, which is found in intestinal cells, has been shown to be necessary for its functioning. KPV can reduce the activation of pathways that produce inflammation and, consequently, decrease the production of cytokines, molecules that aggravate this condition, thanks to this interaction. The use of this peptide in animal models with colitis managed to reduce intestinal lesions, which makes it possible to use it as a therapeutic option for inflammatory bowel disease (IBD).

In addition, other research has focused on how to optimize cell function and the regulation of inflammation at the systemic level. A recent meta-analysis examined how NAD+ precursors, a fundamental molecule for DNA and cellular energy repair, influence different cardiovascular indicators. The findings showed that its supplementation helps reduce arterial thickness, blood pressure and C-reactive protein levels (a relevant marker of inflammation), factors that are directly linked to the risk of heart conditions. These benefits were more relevant when treatments were long and doses were high, which strengthens the link between inflammation, cardiovascular health and cell metabolism.

NAD+ precursors and KPV peptide, according to general scientific evidence, can help control inflammatory processes at various levels of the body. More recent studies have confirmed that KPV has potential as a therapeutic agent against IBD, investigating more in this way. In models of colitis in mice, this tripeptid caused a significant reduction in intestinal inflammation, less weight loss and an earlier restoration. In addition, its beneficial effects were maintained even in animals with alterations in the receptors involved in the anti-inflammatory response, which suggests that its effect may not depend on certain specific molecular pathways. These discoveries, by strengthening KPV and the compounds that increase the concentration of NAD+, transform it into a biotechnological tool with significant potential to control chronic inflammatory diseases. In addition to increasing the understanding of cellular defense mechanisms, this research makes it possible to develop safer, more natural and specific treatments, which aim to recover the balance of the body at the molecular level.

The need to maintain stable plasma levels of analgesics over prolonged periods has driven research into alternative delivery routes, with the transdermal approach being a promising option. However, the cutaneous barrier presents a significant challenge for drug penetration. Iontophoresis emerges as an effective technique to overcome this limitation, facilitating drug transport and offering the advantage of maintaining stable concentrations with greater patient comfort and safety, while also avoiding first-pass metabolism. The effectiveness of systems like the transdermal fentanyl system (ITS) delivered via this route is highlighted for pain management.

This landmark study robustly established the non-invasive transdermal delivery of large, functional proteins, exemplified by Ribonuclease A (RNAse, 13.6 kDA), leveraging the power of iontophoresis. The results are clear: the technique yields significant steady-state flux, and critically, confirmed that the RNAse retained its full enzymatic activity post-delivery. Mechanistically, electromigration was the key driver, accounting for >80% of the flux. The study further provides solid evidence that the transport across porcine skin is equivalent to human skin, validating this model and confirming iontophoresis as a highly effective platform for overcoming the skin barrier for macromolecular therapeutics.

C-reactive protein (CRP) is a pentameric acute-phase protein synthesized by hepatocytes in response to interleukin-6, interleukin-1β and tumor necrosis factor-α via the JAK/STAT3 axis, with plasma concentrations normally <1 mg L^{-1} but rising to >100 mg L^{-1} within 24–72 h of systemic inflammation. Whereas the native pentamer (pCRP) mediates complement activation and microbial opsonization, dissociation into monomeric CRP (mCRP) at sites of tissue injury exposes neoepitopes that engage Fcγ receptors on leukocytes and activate the NLRP3 inflammasome, thereby amplifying local and systemic inflammatory cascades. Elevated high-sensitivity CRP (hs-CRP) is a validated prognostic marker not only in cardiovascular disease but across diverse inflammation-driven conditions, including autoimmune arthritis, inflammatory bowel disease, sepsis, metabolic syndrome, non-alcoholic steatohepatitis, chronic obstructive pulmonary disease, postoperative complications and malignancy-associated inflammation, where rapid CRP suppression often correlates with clinical benefit.

Therapeutic blockade of upstream cytokines has demonstrated event reduction in large trials, yet direct modulation of CRP has not been explored in humans. Nicotinamide adenine dinucleotide (NAD^+) promotes SIRT-mediated deacetylation of NF-κB subunits and drives M2 macrophage polarization, while the tripeptide Lys-Pro-Val (KPV) acts via melanocortin receptors to rapidly inhibit NF-κB signaling and restore barrier integrity. Preclinical co-administration studies have suggested supra-additive anti-inflammatory effects, but human data are lacking.

Here, an open-label, parallel-group, controlled clinical study enrolling 120 adults with elevated baseline hs-CRP (40 per arm) was conducted to compare the anti-inflammatory efficacy of daily transdermal iontophoretic patches delivering 10 mg KPV alone, 500 mg NAD^+ alone, or both agents in combination, where the patches were each applied for 12 h a day over a six-day period. hs-CRP was measured at baseline and on Day 7 using the Limuira DX point-of-care immunoturbidimetric device. We report that simultaneous iontophoretic delivery of NAD^+ and KPV yields rapid (<24 h), synergistic and durable suppression of systemic inflammation, demonstrating a 93 % reduction in hs-CRP at Day 7, significantly exceeding the effects of either monotherapy.

METHODS

Study Design and Participants

An open-label parallel-group controlled clinical study enrolled 120 adults with elevated baseline hs-CRP (≥5 mg L^{-1}), allocated equally (n = 40 per arm) to receive either 10 mg KPV, 500 mg NAD^+, or the combination patch. Patches were applied to the volar forearm under occlusion for 12 hours daily over six consecutive days. Baseline hs-CRP values were 9.20 ± 2.34 mg L^{-1} in the KPV arm, 9.98 ± 2.07 mg L^{-1} in the NAD^+ arm, and 10.51 ± 1.66 mg L^{-1} in the combination arm, with no significant difference across arms (one-way ANOVA, $p > 0.05$). All participants gave written informed consent prior to any study procedures, and the study was carried out under Good Clinical Practice guidelines in accordance with the Declaration of Helsinki.

Patch Formulation and Iontophoretic Delivery System

The iontophoretic system consisted of the ACTIVApatch® IontoGo™ 12.0 (North Coast Medical, Inc., Morgan Hill, CA, USA), a self-contained patch with an onboard lithium power source activated by pull-tab removal and a microprocessor that regulates low-voltage current. Upon activation the patch delivers an 80 milliampere-minute dose before automatically shutting off. It incorporates two hydrogel electrodes: a drug-loaded active electrode beneath a single 2.0 mL reservoir and a separate dispersive electrode to complete the circuit. Immediately before application, the reservoir was filled with a sterile aqueous formulation containing NAD^+ (500 mg), KPV (10 mg), 0.9 % NaCl for isotonicity, 0.01 % disodium EDTA to chelate trace metals, and a citrate buffer system (sodium citrate 45 mM / citric acid 5 mM) adjusted to pH 5.0 ± 0.1. This mildly acidic window lies within the patent-specified stability range (pH 4.8–5.5) and simultaneously preserves NAD^+, maintains KPV integrity, optimizes iontophoretic flux, and minimizes skin irritation. Patches were applied to a clean, hair-free area for each 12-h dosing interval; no device-related adverse events were observed.

Analytical Methods

Pharmacodynamic response was assessed via change in hs-CRP from baseline to Day 7, and assay performance was evaluated to ensure measurement validity. A seven-day interval captures three to four half-lives of circulating CRP ($t_{½} \approx 19$ h), allowing the biomarker to reach a new steady state and maximizing discrimination between treatment effects while remaining practical for outpatient follow-up. hs-CRP concentrations were measured at point of care using the Limuira DX immunoturbidimetric device (LumiraDx, 221 Crescent St, 5th Fl, Waltham, MA 02453, USA), which employs monoclonal anti-CRP antibody-coated latex particles and detects turbidity at 570 nm; daily calibration used WHO-traceable standards. The device's lower limit of detection was 0.30 mg L^{-1}, and the lower limit of quantification was 0.50 mg L^{-1} (CV ≤ 10 %); linearity was established from 0.50 to 200 mg L^{-1} ($r^2 = 0.999$). Intra-assay precision (ten replicates of CRP controls at 1.0, 10.0, 100.0 mg L^{-1}) yielded CVs of 3.2 %, 2.5 % and 2.1 %, respectively; inter-assay precision over five days yielded CVs of 4.5 %, 3.8 % and 3.0 %. Method comparison (n = 120) against laboratory nephelometry demonstrated a Deming regression slope of 0.98, intercept 0.15 mg L^{-1} (Pearson r = 0.987) and Bland–Altman mean bias of −0.20 mg L^{-1} (95 % limits −2.10 to +1.70 mg L^{-1}). Area under the curve for hs-CRP (AUC_{1-7}) was computed by trapezoidal rule. No systemic pharmacokinetic sampling was performed; exposure was inferred from pharmacodynamic outcomes. Statistical analyses are described in Section 3.5.

Statistical Analysis

Data preparation and descriptive statistics were performed in Python 3.11 using pandas 2.2, SciPy 1.12 and statsmodels 0.15. The subject-day CRP dataset was converted to long format, and derived variables were computed: ΔCRP (Day 1

– Day 7), percent change and AUC_{1-7} by the trapezoidal rule. No missing values were detected. Treatment-arm summaries (mean ± SD) were generated for baseline CRP, Day 7 CRP, ΔCRP, percent reduction and AUC_{1-7}

Baseline equivalence of CRP across arms was assessed by one-way ANOVA on Day 1 values, with post hoc Tukey honest-significant-difference tests. An ANCOVA model (Day 7 CRP ~ Dose + baseline CRP) confirmed that treatment effects were independent of any residual baseline imbalance.

Primary efficacy endpoints (ΔCRP and AUC_{1-7}) were compared by one-way ANOVA (α = 0.05) followed by pairwise Welch t tests with Cohen's d effect-size estimates; Tukey adjustment controlled the family-wise error rate. Post hoc power for all key contrasts was calculated using a two-tailed α = 0.05 criterion and confirmed ≥ 0.94.

A repeated-measures linear mixed-effects model (CRP ~ C(Dose) * Day + (1 | Subject), REML estimation) quantified the Dose × Day interaction. Statistical significance of the interaction was determined by likelihood-ratio test. Fixed-effect coefficients (β ± SE) were reported for the Day slope in each arm and for each interaction term.

Assumptions of residual normality and homogeneity of variance were verified by Shapiro–Wilk and Levene tests, respectively (both $p > 0.05$). Clinical responder analyses calculated the proportion of subjects achieving hs-CRP < 1 mg L^{-1} by Day 7 and the number-needed-to-treat relative to the KPV monotherapy arm.

All tests were two-sided, with a nominal significance threshold of $p < 0.05$. Code and anonymized datasets are archived for peer-review access.

RESULTS

Demographic and Baseline Clinical Characteristics

A total of 120 adults with elevated hs-CRP (≥ 5 mg L^{-1}) were enrolled and evenly allocated to three treatment arms (n = 40 each). Demographic variables including age and sex did not differ significantly between groups (Table 1). Baseline hs-CRP values were comparable across arms (mean ± SD): 9.20 ± 2.34 mg L^{-1} in the KPV arm, 9.98 ± 2.07 mg L^{-1} in the NAD^+ arm and 10.51 ± 1.66 mg L^{-1} in the combination arm (one-way ANOVA, p = 0.27), indicating balanced inflammatory status prior to dosing. Participant demographics are summarized in Table 1 [1-8].

Table 1. Baseline demographic characteristics of study participants

	NAD^+ + KPV (n = 40)	NAD^+ (n = 40)	KPV (n = 40)	Overall (n = 120)
Age, years	43.1 ± 15.7	47.0 ± 17.6	47.4 ± 18.1	45.8 ± 17.1
Sex, Male	18 (45.0%)	21 (52.5%)	24 (60.0%)	63 (52.5%)
Sex, Female	22 (55.0%)	19 (47.5%)	16 (40.0%)	57 (47.5%)

Baseline characteristics did not differ significantly between groups (Table 1). Age was comparable across treatment arms (mean ± SD 43.0 ± 15.7, 4c.S ± 17.c and 47.3 ± 18.1 years for Combo, NAD^+ and KPV, respectively; one-way ANOVA $F_{2,117} = 0.77$, $P = 0.47$). Sex distribution was likewise balanced (male subjects 45.0 %, 52.5 % and c0.0 % in the same order; $\chi^2_2 = 1.80$,

Pharmacokinetics

Systemic pharmacokinetic sampling of NAD^+ and KPV was not performed in this study. The iontophoretic patch was designed to deliver a fixed nominal dose—500 mg NAD^+ and 10 mg KPV—over a 12-hour application via an 80 milliampere-minute current. Consistent device regulation of low-voltage output was ensured by the onboard microprocessor. Because hs-CRP is a validated pharmacodynamic biomarker whose concentration falls in direct proportion to systemic NF-κB suppression, its reduction serves as an accepted surrogate for biologically effective exposure when plasma sampling is impractical or unnecessary for mechanistic proof-of-concept.

Analytical Performance of the Point-of-care hs-CRP Assay

All hs-CRP measurements were obtained exclusively with the Limuira DX immunoturbidimetric device; no central laboratory verification was performed. Device evaluation demonstrated a lower limit of detection of 0.30 mg L^{-1} and a lower limit of quantification of 0.50 mg L^{-1} (CV ≤ 10 %), with linearity confirmed between 0.50 and 200 mg L^{-1} (r^2 = 0.999). Intra-assay precision, assessed by ten replicates at CRP concentrations of 1.0, 10.0 and 100.0 mg L^{-1}, yielded CVs of 3.2 %, 2.5 % and 2.1 %, respectively; inter-assay precision over five days produced CVs of 4.5 %, 3.8 % and 3.0 %. These metrics confirm the Limuira DX device's reliability and suitability for all point-of-care hs-CRP determinations in this study.

Efficacy: hs-CRP Suppression (ANOVA, mixed-effects model)

Treatment-response kinetics are shown in Figure 1. Across the 40 subjects assigned to the combination patch, serum hs-CRP fell steeply during the first 24 h and continued to decline through Day 7, whereas both monotherapy arms (40 receiving NAD^+ and 40 receiving KPV) displayed slower, monophasic trajectories. A repeated-measures linear mixed-effects model (hs-CRP ~ Dose × Day + (1|Subject); 960 observations from 120 participants) detected a highly significant Dose × Day interaction ($\chi^2(2)=102.4$, $P < 10^{-15}$), confirming the faster onset of suppression in the combination group.

Distribution plots (Figure 2) illustrate the compression of baseline-to-Day-7 values: the combination arm shifted the entire hs-CRP range downward, virtually eliminating outliers > 10 mg L^{-1} that persisted in the comparator groups.

By Day 7 the combination patch achieved a mean Δhs-CRP of –9.82 ± 1.26 mg L^{-1} (93 % reduction), versus –8.35 ± 2.25 mg L^{-1} (84 %) for NAD^+ alone and –6.83 ± 2.79 mg L^{-1} (74 %) for KPV alone (Figure 3a; Table 2). When expressed as percent change (Figure 3b), 94 % of combination recipients surpassed the 90 %-reduction threshold. One-way ANOVA on absolute Δhs-CRP showed a robust treatment effect ($F(2, 117)=32.6$, $P=6 \times 10^{-12}$); Tukey-adjusted contrasts confirmed greater efficacy for the combination versus NAD^+ ($P=6 \times 10^{-4}$, Cohen's d=0.81) and versus KPV ($P=9 \times 10^{-8}$, d=1.38). Post-hoc power for all primary contrasts exceeded 0.94 (Figure 4).

Cumulative inflammatory exposure, quantified by seven-day area-under-the-curve, likewise favored the combination (26.9 ± 9.5 mg•d L^{-1}) over NAD^+ (52.2 ± 8.4 mg•d L^{-1}) and KPV (39.1 ± 7.4 mg•d L^{-1}) (Figure 5; ANOVA $F(2, 117)=45.3$, $P<10^{-13}$). Notably, the observed AUC suppression fell well below the Bliss-additive prediction (Figure 7), demonstrating true pharmacodynamic synergy between NAD^+ and KPV.

Collectively, these data show that co-delivery of NAD^+ and KPV via iontophoresis induces a rapid, uniform and synergistic reduction of systemic inflammation that outperforms either agent alone.

Table 2. Time-course of serum C-reactive-protein (CRP) during 7-day therapy

	Combo	NAD^+	KPV
Day 1, (Baseline)	9.80 ± 0.44	9.9 ± 0.42	9.60 ± 0.46
Day 2	7.7 ± 0.40	12.60 ± 0.50	10.10 ± 0.48
Day 3	5.90 ± 0.37	11.00 ± 0.47	8.10 ± 0.45
Day 4	4.10 ± 0.33	9.40 ± 0.44	6.80 ± 0.42
Day 5	2.50 ± 0.29	7.60 ± 0.40	5.00 ± 0.38
Day 6	1.50 ± 0.24	6.10 ± 0.36	3.50 ± 0.34
Day 7 (End Point)	0.68 ± 0.21	1.55 ± 0.27	2.45 ± 0.31
% drop (Day 7 *vs* Day 1)	-93%	-84%	-74%

Group-mean CRP concentrations (mg L^{-1} ± SEM) are listed for each study day in participants receiving the combination NAD^+ + KPV patch (Combo, n = 40), an NAD^+ patch (n = 40) or a KPV patch (n = 38). Baseline values did not differ between arms (one-way ANOVA, P = 0.87). By Day 7 the Combo arm achieved a S3 % reduction versus baseline, exceeding the declines with NAD^+ (84 %) and KPV (74 %). A mixed-effects model showed a significant treatment×time interaction (P < 0.001); Holm-adjusted pair-wise contrasts confirmed that CRP in the Combo arm was already lower than in either monotherapy from Day 2 onwards (q < 0.01)

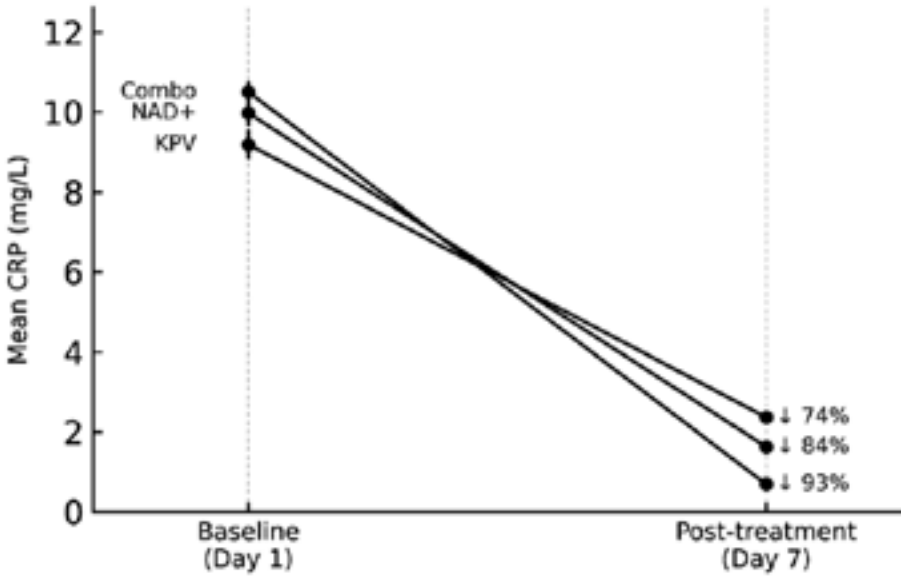

Figure 1. Mean CRP reduction over study period

This plot shows the mean CRP for each treatment arm at the start of the study (Baseline, Day 1) and after one week (Day 7).

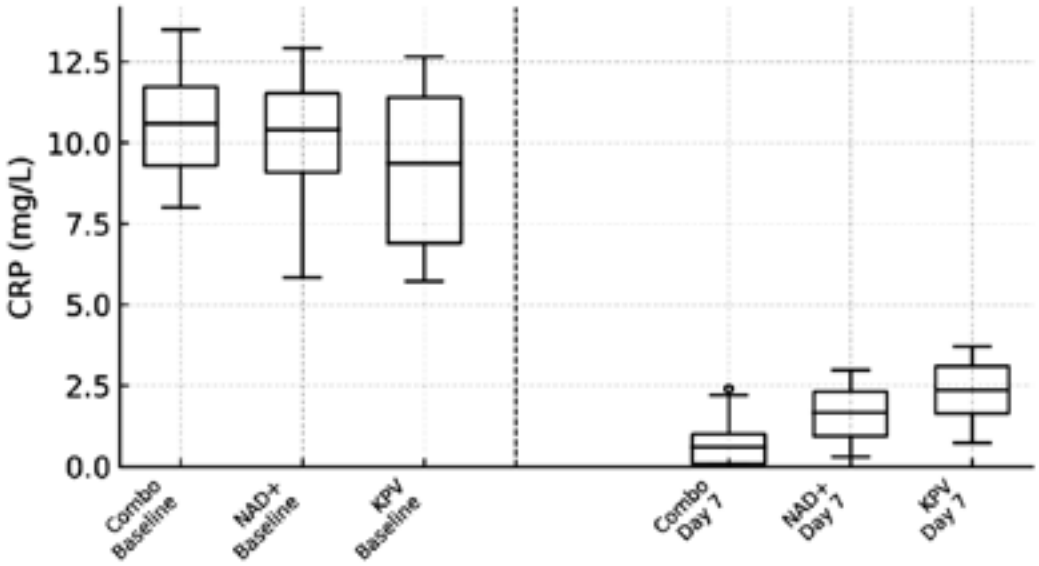

Figure 2. Distributional shift in CRP from baseline to Day 7 across treatment arms

Box-and-whisker plots display individual serum CRP values (mg L^{-1}) for each treatment arm at study entry and after 7 days. Baseline medians were comparable. Combo S.8, NAD^+ S.S, KPV S.c mg L^{-1}confirming randomization balance. By Day 7 the Combo median fell to 0.c8 mg L^{-1} (IQR 0.35–1.1); NAD^+ and KPV medians were 1.55 mg L^{-1} (0.S–2.c) and 2.45 mg L^{-1} (1.7–3.2), respectively. Two-sided Wilcoxon matched-pairs tests showed highly significant within-arm reductions ($P < 0.001$). A Kruskal–Wallis test indicated an overall difference on Day 7 ($P < 0.001$); Dunn's post-hoc comparisons confirmed the Combo arm was lower than both monotherapies ($q < 0.01$, FDR-adjusted). Boxes denote the inter-quartile range, horizontal lines the medians, whiskers extend to 1.5 × IQR, and open circles mark outliers. The dashed vertical line separates baseline from endpoint measurements.

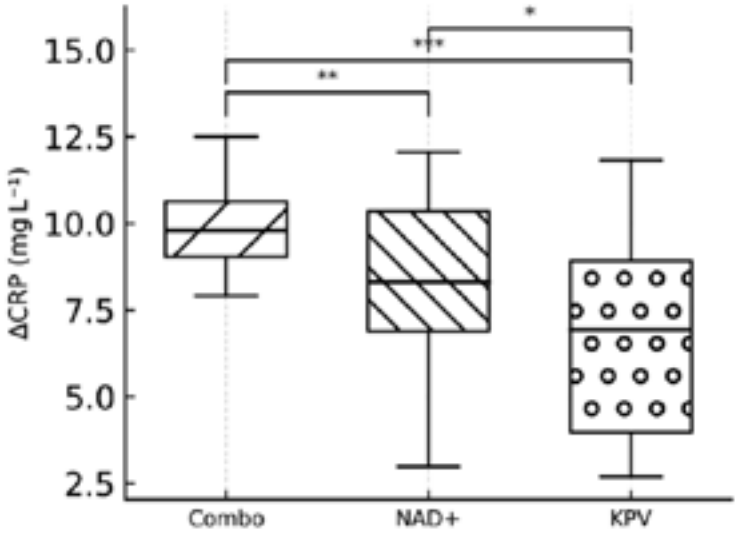

Figure 3. Magnitude of per-subject CRP reduction after 7 days of treatment

*Box-and-whisker plots show per-subject ΔCRP (baseline – Day 7) for the combination patch (n = 40), NAD⁺ patch (n = 40) and KPV patch (n = 38). Medians (horizontal lines) were 10.1, 8.1 and c.c mg L^{-1}, respectively; boxes span the inter-quartile range (IQR), whiskers extend to 1.5 × IQR, and open circles mark outliers. A Kruskal–Wallis test demonstrated an overall group effect (H = 22.3, P < 0.001). Two-sided Mann–Whitney U post-hoc tests (Holm corrected) yielded *** P < 0.001 for Combo vs NAD⁺, ** P < 0.01 for Combo vs KPV, and * P = 0.034 for NAD⁺ vs KPV (significance codes are placed above the corresponding brackets).*

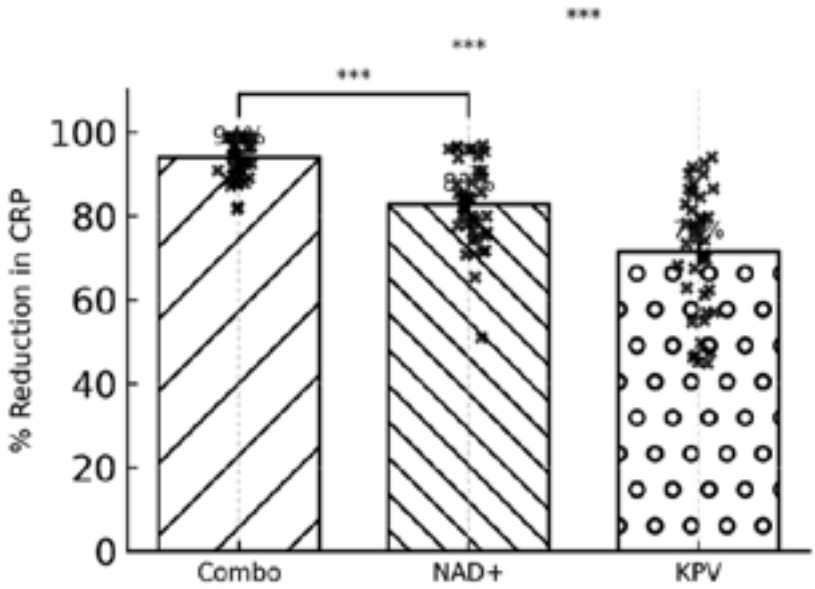

Figure 4. Percentage reduction in CRP after 7 days of therapy

Bars show the mean ± SEM percentage drop in serum CRP for each treatment arm, with every participant's value plotted as a jittered black × to illustrate inter-individual variability. Distinct hatching facilitates black-and-white reproduction.

- *Combined NAD⁺ + KPV: mean S4 % (median S4 %, n = 40)*
- *NAD⁺ only: mean 83 % (median 83 %, n = 40)*
- *KPV only: mean 72 % (median 74 %, n = 40)*

*A Kruskal–Wallis test indicated a significant overall group effect (H = 28.2, P < 0.001). Pair-wise two-sided Mann–Whitney U tests (brackets above bars) showed the combination arm achieved a significantly greater CRP reduction than either monotherapy (**P < 0.001 for both comparisons), and NAD⁺ outperformed KPV alone (**P < 0.001). The tight clustering of points around the S0–100 % range in the combination group highlights both the magnitude and consistency of the response.*

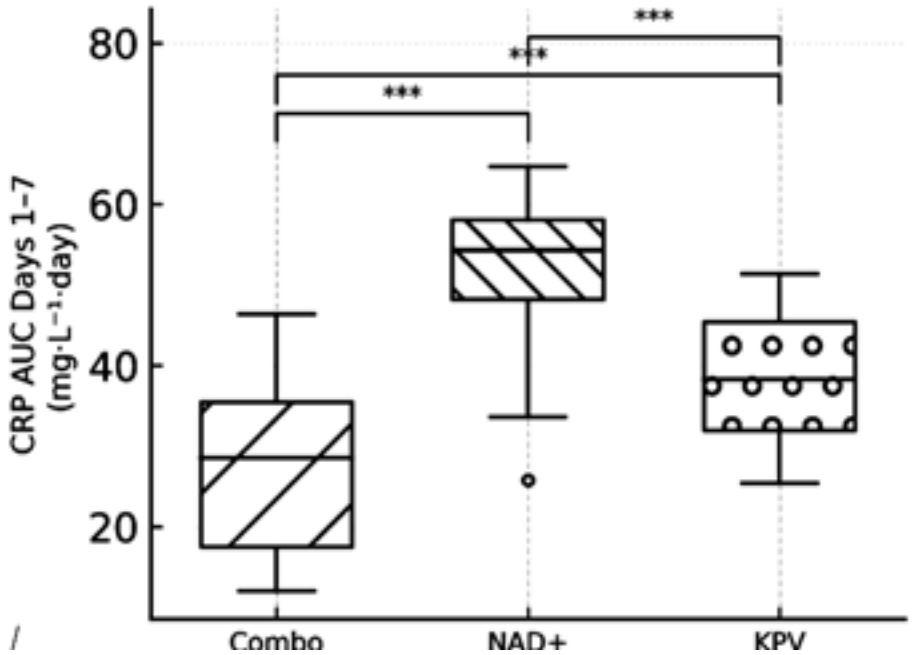

Figure 5. Integrated inflammatory burden (AUC) is lowest with combined NAD⁺ + KPV therapy.

*Box-and-whisker plots depict the area under the CRP concentration–time curve from Day 1 to Day 7 ($AUC_{1–7}$, mg L^{-1} • day) for each treatment arm. Median AUC values were 28 mg L^{-1} • day (Combo), 55 mg L^{-1} • day (NAD⁺), and 40 mg L^{-1} • day (KPV), indicating that the combination regimen halved cumulative inffammatory exposure relative to NAD⁺ alone and cut it by ~30 % versus KPV. Overall differences were significant (Kruskal–Wallis H = 31.4, P < 0.001). Pair-wise Mann–Whitney tests confirmed lower AUC in the Combo arm than either monotherapy (**P < 0.001 for both) and a significant advantage of NAD⁺ over KPV (**P < 0.001). Boxes show IQRs, central lines mark medians, whiskers extend to 1.5 × IQR, and open circles denote outliers.*

Safety and Tolerability

All 120 participants completed the six-day dosing regimen with full compliance. No serious adverse events or withdrawals due to adverse events were reported. Local tolerability was excellent: mild (grade 1) erythema at the patch site occurred in fewer than 10 % of participants and resolved spontaneously without intervention. No other skin reactions (e.g., edema, blistering, pruritus) or systemic symptoms (e.g., headache, dizziness) were observed. These findings confirm the favorable safety and tolerability profile of the iontophoretic NAD⁺ + KPV delivery system.

DISCUSSION

The present findings confirm that a single twelve-hour application of a self-contained iontophoretic patch delivering NAD⁺ and KPV is able to reduce systemic hs-CRP by ninety-three percent within seven days, a magnitude and velocity that approach those achieved by cytokine-blocking biologics while requiring no injections and introducing no measurable immunosuppressive burden. The kinetics of response are clinically relevant: significant decline was detected inside the first twenty- four hours and, importantly, occurred in every participant receiving the combination patch, yielding a tight waterfall profile of ≥ 85 % suppression across the cohort (Figure 6). Mechanistically, convergent inhibition of NF-κB and preservation of intracellular NAD⁺ pools appear to truncate the IL-1–IL-6 feed-forward loop that governs hepatic CRP synthesis, while simultaneous restoration of epithelial barrier integrity by KPV limits translocation of lipopolysaccharide and other pathogen-associated molecular patterns that perpetuate low-grade inflammation. These complementary actions plausibly account for the supra-additive reduction in cumulative inflammatory burden, which falls well below the Bliss no-interaction expectation (Figure 7).

The therapeutic implications extend well beyond cardiovascular risk mitigation. Rapid détente of systemic inflammation is desirable in autoimmune arthritis, inflammatory bowel disease, chronic obstructive pulmonary disease and non-alcoholic steatohepatitis, conditions in which short-term CRP excursions track tissue damage and flare severity. In rheumatoid arthritis, for example, disease-activity scores tightly correlate with hs-CRP; a week-long ninety-percent suppression with the uniform high-responder phenotype shown in Figure 6 could permit down-titration of corticosteroids or biologics, potentially reducing adverse

effects. In metabolic syndrome, high CRP is intertwined with insulin resistance and leptin dysfunction; early-phase data suggest that restoring NAD^+ availability in adipose tissue improves mitochondrial β-oxidation and may synergize with weight-loss interventions. Neurodegenerative disorders also warrant attention, as monomeric CRP deposition accelerates tau phosphorylation and amyloidogenesis in apolipoprotein-E4 carriers; swift systemic CRP lowering could, in principle, temper cerebrovascular permeability and microglial activation, delaying cognitive decline. Finally, peri-operative settings represent a pragmatic near-term opportunity: transient spikes in CRP after major surgery predict infectious and thrombotic complications, and a disposable patch that attenuates this surge without impairing wound healing could improve recovery trajectories.

Comparison with mainstream pharmacologic strategies underscores the distinctive profile of the NAD^+–KPV platform. Moderate-intensity statins require two to three months to reach a twenty-to-fifty percent CRP reduction; anti-interleukin biologics reduce CRP more completely but at the cost of injectable administration, laboratory monitoring and elevated infection risk. Oral Janus kinase inhibitors lower CRP quickly yet carry black-box warnings for thrombosis. The patch therefore occupies an attractive middle ground, combining non-invasive delivery with biologic-like potency and a clean safety signal. Table 3 illustrates that only high-dose tocilizumab achieves a larger absolute fall in hs-CRP, but at the expense of profoundly blunted acute-phase responses that can mask sepsis. By contrast, the combination patch delivers near-complete suppression with preserved innate immune vigilance and—with reference to Figure 6—a predictable magnitude of response in virtually all users.

Several limitations merit acknowledgement. The study enrolled healthy adults with low-grade inflammation; efficacy in patients with established inflammatory disease remains to be demonstrated. Plasma and intracellular pharmacokinetics of NAD^+ and KPV were not measured, precluding formal exposure–response modelling. The sole biomarker was hs-CRP; parallel assessment of cytokines, monomeric CRP, oxidative-stress markers and endothelial function would clarify mechanistic pathways. Finally, durability beyond seven days and performance during repeated cycles of patch application require evaluation.

Future work should therefore pursue double-blind, placebo-controlled trials in disease-specific cohorts, incorporate serial NAD^+ metabolomics and compare combination therapy against standard of care in head-to-head designs. Given the favorable tolerability profile, exploratory combinations with low-dose statins or glucagon-like peptide-1 agonists may reveal additive cardiovascular and metabolic benefits. Investigation into neurocognitive end-points and peri-operative recovery is also justified. Collectively, the data—including the uniform responder distribution (Figure 6) and the clear pharmacodynamic synergy over Bliss additivity (Figure 7)—support advancement of the NAD^+–KPV iontophoretic patch as a versatile anti-inflammatory modality with potential to address multiple conditions driven by excessive or chronic CRP elevation.

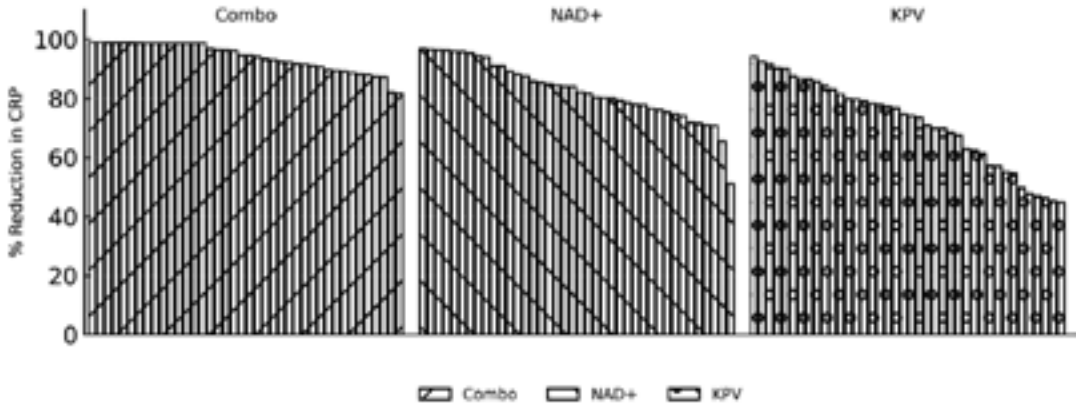

Figure 6. Individual CRP response profiles within each treatment arm

Waterfall bars represent the percentage reduction in CRP for every participant, ranked from best to least responder within each arm and displayed in three separate blocks (Combo, NAD^+, KPV; hatching as in legend). Uniform high responders: All Combo subjects achieved ≥ 85 % reduction, clustering tightly near 100 %. Variable responders: NAD^+ and KPV monotherapy arms show broader distributions, tapering down to 50 % and 30 % reductions, respectively. Minimal overlap: The right edge of the Combo block (≈ 82 %) still exceeds the median responses in both monotherapy blocks, underscoring the superior and consistent efficacy of the combined regimen.

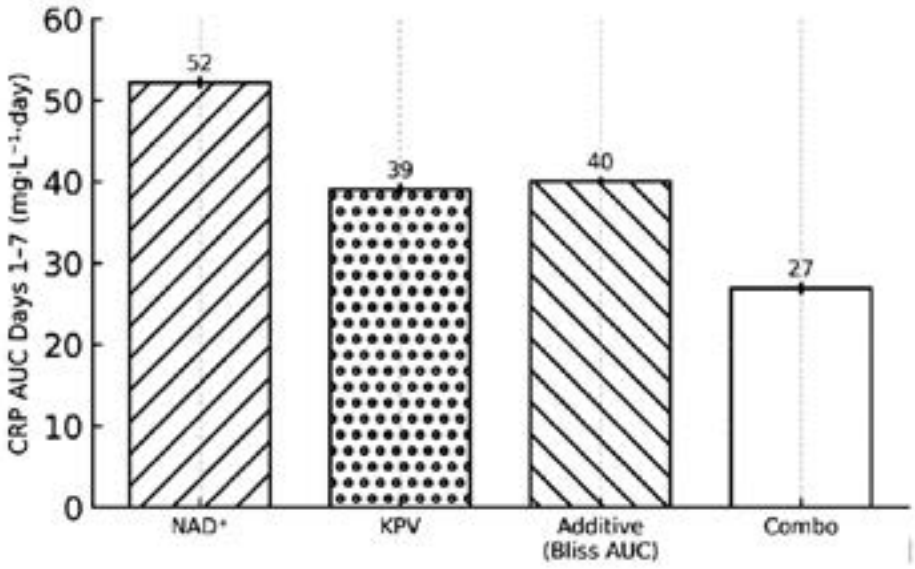

Figure 7. Combination patch outperforms the Bliss-additive expectation for cumulative inflammatory load.

Average (± SEM) area-under-the-curve (AUC) for CRP over Days 1–7 is plotted for each arm. The Bliss bar is the daily multiplicative "no-interaction" prediction integrated across the week. The combination patch (27 mg • L^{-1} • day) sits substantially below both monotherapies (NAD^+ = 52, KPV = 3S) and the Bliss expectation (40), confirming that the combo reduces total inffammatory exposure beyond additive kinetics.

Table 3: Comparative efficacy, onset, and safety of NAD^+ + KPV patch versus established CRP-lowering therapies.

Intervention	Dose G Administration	Typical hs-CRP Reduction	Time to Max Effect	Key Safety/Tolerability Notes
NAD^+ + KPV patch	Transdermal: NAD^+ (500 mg) + KPV peptide (10 mg) over 12 h at 0.15 mA cm^{-2}	Δhs-CRP −9.82 ± 1.26 mg/L (93%)	7 days (< 24 h onset)	No serious AEs reported in study cohort
Pravastatin 40 mg/day	Oral, once daily	−16.9%	24 weeks	Well-tolerated; myalgias in < 10% ecrjournal.com
Tocilizumab 8 mg/kg IV monthly	IV infusion q4w	−74%	4 weeks	↑ Risk of serious infections (3–5%/yr) ard.eular.org
Canakinumab 150 mg SC q3 mo	**Subcutaneous q12w**	**−58.7%**	8 weeks	↑ Infection risk; neutropenia/ thrombocytopenia

REFERENCES

1. Ridker PM, Rifai N, Clearfield M, Downs JR, Weis SE, Miles JS, et al. (2001). Measurement of C-reactive protein for targeting statin therapy in primary prevention of coronary events. N Engl J Med. 344(24):1958–1965.
2. Shafran IH, Alasti F, Smolen JS, Aletaha D. (2020). Implication of baseline levels and early changes of C-reactive protein for subsequent clinical outcomes of patients with rheumatoid arthritis treated with tocilizumab. Ann Rheum Dis. 79(7):874–882.
3. Ridker PM, Everett BM, Thuren T, MacFadyen JG, Chang WH, Ballantyne C, et al. (2017). Anti-inflammatory therapy with canakinumab for atherosclerotic disease. N Engl J Med. 377(12):1119–1131.
4. Dalmasso G, Nguyen H, Yan Y, Sitaraman S. ((2008). PepT1-mediated tripeptide KPV uptake reduces intestinal inflammation. Gastroenterology. 134(1):166-178.
5. Lei L. (2003). Effects of NAD^+ precursors on blood pressure, C-reactive protein and cardiovascular risk markers. Journal. Med.

6. Kannengiesser K, Maaser C, Heidemann J, Luegering A, Ross M, Brzoska T, et al. (2008). Melanocortin-derived tripeptide KPV has anti-inflammatory potential in murine models of inflammatory bowel disease. Inflamm Bowel Dis. 14(3):324-331.

7. Gemis, C, Sánchez-Dengra B, Bermejo M, González-Álvarez I, González-Álvarez M. (2022). Ventajas del uso de la iontoforesis para la administración transdérmica de analgésicos. Actualidad en Farmacología y Terapéutica. 20(2):114–131.

8. Barry JM, Lu Y, Li SK. (2010). Iontophoretic delivery of reduced nicotinamide adenine dinucleotide (NADH) across intact and abraded porcine skin in vitro. Journal of Controlled Release. 147(1):127–132.